Year: 2021

A multispectral design for a new generation of film scanners

Trumpy, Giorgio ; Hardeberg, Jon Y ; George, Sony ; Flueckiger, Barbara

DOI: https://doi.org/10.1117/12.2592655

Originally published at:
Trumpy, Giorgio; Hardeberg, Jon Y; George, Sony; Flueckiger, Barbara (2021). A multispectral design for a new generation of film scanners. In: Optics for Arts, Architecture, and Archaeology VIII, 117840Z, Online-Konferenz, 8 July 2021, SPIE - International Society for Optical Engineering.
DOI: https://doi.org/10.1117/12.2592655

A multispectral design for a new generation of film scanners

Trumpy, Giorgio, Hardeberg, Jon Y., George, Sony, Flueckiger, Barbara

Giorgio Trumpy, Jon Y. Hardeberg, Sony George, Barbara Flueckiger, "A multispectral design for a new generation of film scanners," Proc. SPIE 11784, Optics for Arts, Architecture, and Archaeology VIII, 117840Z (8 July 2021); doi: 10.1117/12.2592655

SPIE. Event: SPIE Optical Metrology, 2021, Online Only

A multispectral design for a new generation of film scanners

Giorgio Trumpy[a,b], Jon Y. Hardeberg[b], Sony George[b], Barbara Flueckiger[a]
[a] University of Zurich, Affolternstrasse 56, 8050 Zurich, Switzerland;
[b] Norwegian University of Science and Technology, Teknologivegen 22, 2815 Gjøvik, Norway

ABSTRACT

The digital reproduction of a historical motion picture should resemble as much as possible the analog film projection at the time of the movie release. Nowadays, practices of capturing digital images of films do not properly consider the fundamental elements and conditions of the original film projection. The typical rigid three-band (RGB) capture cannot adapt to the multitude of historical color film stocks to be digitized, and the diffuse illumination on the film generally used by standard digital scanning devices is unable to guarantee the proper visual rendition of the original analog projection of film prints. In order to overcome these problems, we designed and built a novel multispectral imaging system that illuminates the film with a condensed light beam. The new imaging system and the computational pipeline were tested on an assorted set of photographic colors. The accuracy of the multispectral captures was tested by comparison with corresponding spectrally resolved point-based radiometric measurements of the light reflected by a screen during analog projection. The presented optical design represents an excellent solution for the creation of a new multispectral motion picture scanner prototype. The LED-based illumination system coupled with a film transport mechanism can be the core concept of a promising new generation of motion picture film scanners.

Keywords: Multispectral imaging, photographic film, light scattering, film projection

1. INTRODUCTION

Many professional film scanners that are widely used nowadays in the digitization of archival films were primarily conceived to excel in the *Digital Intermediate* workflow of contemporary film productions,[1] and their optical configuration is therefore optimized for chromogenic negative film stock of recent production. In general, commercial film scanners are not compatible with the optical properties of the vast variety of film processes that constitute the holdings of public archives and private film collections. The inaccuracies of the digital scans can be later adjusted at a color grading suite during an analog/digital simultaneous screening, but this operation—if it is ever possible—is time consuming, and its result depends on the judgment and knowledge of operators performing it.[2]

1.1 Current limitation #1 – image capture with rigid RGB bands

Conventional film scanners have three fixed spectral bands located in the long, medium and short ranges of the visible wavelengths—i.e., red, green and blue. The scanners can be ascribed to two categories according to the widths of their spectral bands, such as illustrated in Figure 1. On the one hand, there are spectral bands that do not overlap, aiming at the absorption peaks of typical dyes of modern chromogenic films (cyan, magenta and yellow); these *narrow bands* are conceived to minimize the influence of the film dyes' side absorptions and maximize the digital color information.[3] On the other hand, there are spectral bands that largely overlap; these *broad bands* are conceived to resemble the human visual system and aim at accurate colors. These fixed categories represent a strong limitation for the digitization of film colors, as some types of film should be digitized aiming at the maximum digital color information, while the color accuracy is most important for other types. For example, it is preferable to digitize a faded chromogenic film with narrow bands, as this offers a more effective digital restoration. The example reported in Figure 1 shows the result of digital unfading with one-dimensional look-up tables that do not manipulate the color saturation. The restored colors resulting from the narrow bands are much more vivid. However, the enhanced colors produced by the narrow bands become excessive whenever a film has to be reproduced with accurate colors, as is generally the case with well-preserved projection prints.[4] In addition, the low sensitivity around 600 nm of all three narrow bands creates dangerous "blind spot" (the gray range in the plot of Figure 1). The absorption of some cyan tinting dyes used in the early 20th century is found to be in this spectral region, resulting in digital images in which the cyan is vanished.[1]

In view of all this, none of the RGB scanners available on the market is suitable for all types of film colors. For this reason, the present work proposes a multispectral approach for film scanning.

Optics for Arts, Architecture, and Archaeology VIII, edited by Haida Liang, Roger Groves, Proc. of SPIE Vol. 11784, 117840Z · © 2021 SPIE · CCC code: 0277-786X/21/$21 · doi: 10.1117/12.2592655

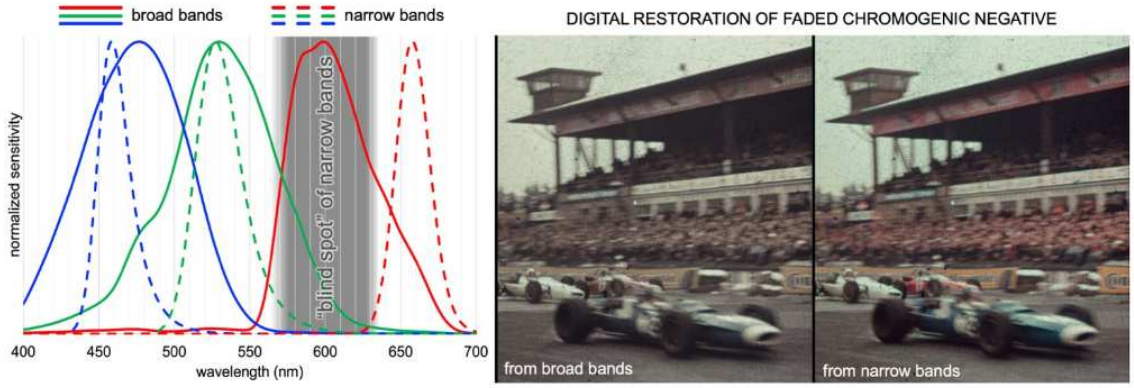

Figure 1. Left: Comparison between the typical broad (solid lines) and narrow spectral bands (dashed lines) of conventional film scanners. Right: Comparison between the result of digitally restoring the color of a faded film frame from an image capture with broad bands (left image) and from an image capture with narrow bands (right image).

1.2 Current limitation #2 – image capture in diffuse illumination

Another serious limitation of all conventional film scanners is their illumination method that does not properly reflect the conditions of film projection. To guarantee a sufficient brightness on the screen of cinema theaters, film projectors employ parabolic mirrors or condensers that direct the light into the lens that images the photographic emulsion on the screen. This highly directional arrangement of light rays is called *condensed* illumination. On the other hand, all most popular film scanners capture photographic images illuminating the film with a light diffuser (opal glass or integrating sphere). The *diffuse* illumination has the important advantage of attenuating the dark marks of dust and scratches on the film,[5] but it does not conform with the way film is illuminated during film projection. In condensed illumination the light hitting the film is concentrated in a small range of angles, while in diffuse illumination the range of light directions covers the full phase space. Films that contain scattering particles, such as tinted and toned films and other early film colors, produce quite different images in diffuse and condensed illumination: the condensed illumination creates an image with deeper darks and more evident grain, while the diffuse illumination creates an image with lower global and local contrast.[6] Film toning exhibits the most significant difference between the two illumination types. If the diffuse/condensed discrepancy is not properly taken into consideration, early film colors risk to be improperly digitized and their digital version will not match the appearance of the original analog projection.[7]

2. A NEW OPTICAL DESIGN

To overcome the limitations reported in the introduction, a multispectral imaging system was designed and built, serving as a prototype of a new film scanner that can produce the most suitable digital image for all types of historical film.

In the presented imaging system, the multispectral capture comprises a set of evenly distributed narrow spectral bands that cover the whole visible spectral range. Three bands of the set correspond to the conventional red, green and blue narrow bands described in the introduction (the dashed lines in Figure 1-left). This allows to either enhance the digital color information by selecting the red, green and blue bands only, or make use of all the spectral bands obtaining the most accurate colors. This flexibility allows to properly digitize all types of film colors: well-preserved projection prints as well as faded dyes, non-standard colors of early cinema as well as camera negatives and other intermediate film elements.

The film is illuminated with a condensed beam that resembles the illumination during film projection. The possibility to insert a light diffusing slab close to the film allows to switch between condensed and diffuse illumination. This guarantees another degree of flexibility, thus benefiting from a true-to-projection color rendering, as well as from attenuated marks of dust and scratches. According to the type of film stock and its physical conditions, the scanner operator has the possibility to choose between the two types of illumination. The film scanner also allows to capture each film frame in both diffuse and condensed illumination, thus opening the possibility for image processing procedures that combine the advantages of both illumination conditions.

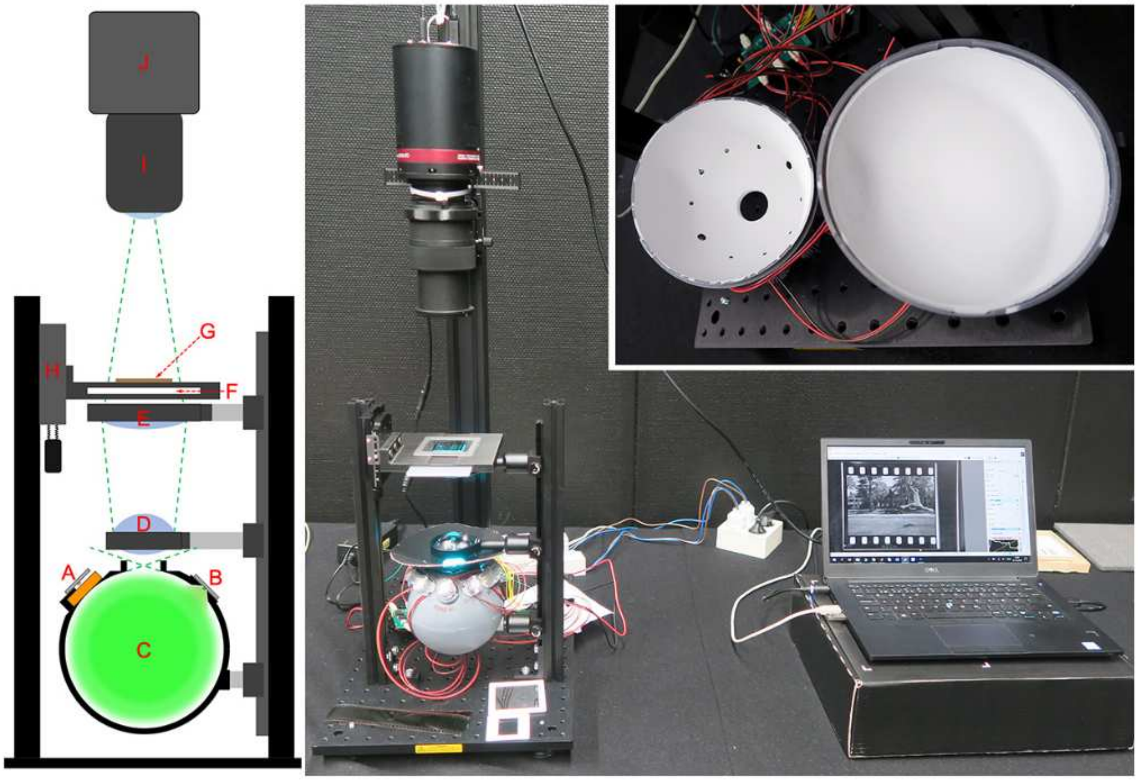

Figure 2. Left: Diagram depicting the integrating sphere (C), one of the LEDs that directly shines into the sphere (B) and one of the LEDs that shines through an interference filter (A). The first (D) and the second condensing lens (E). The sample holder with the light diffusing slab (F), the focusing stage (H) and the film sample (G). The imaging lens (I) and the monochrome camera (J). Right: the complete multispectral imager and the open integrating sphere (inset picture).

For each photographic image, the imaging system captures the spectral images sequentially on an area array sensor. The illumination is provided by a set of light-emitting diodes (LED) whose emissions determine the spectral bands of the imaging system. In order to let all LEDs homogeneously expose the field-of-view with a condensed beam, it was necessary to efficiently bring their light to a common area where the ray bundle of all the LEDs had similar geometry. To achieve this condition without moving parts, a custom-made integrating sphere has been 3D printed in resin (Figure 2), having a 12 cm diameter and whose interior has been sprayed with a nearly-Lambertian reflectance coating. The LEDs shine light inside the sphere through the 4 mm diameter entrance ports (Figure 2, inset picture – the circle of small holes in the top hemisphere). After being scattered, the light comes out from the 2 cm diameter exit port at the top of the integrating sphere. The light coming out from the sphere is collected by a first condensing lens with a numerical aperture of 0.76 that allows to minimize the dispersed light. The second condenser has a diameter of 75 mm and a focal length of 200 mm. The system is configured in such way that the beam is slightly diverging between the two condensing lenses—so to increase the illuminated area—and the image of the sphere's exit port is created approximately where the aperture of the imaging lens is positioned. The camera has a back-illuminated full-frame CMOS monochrome sensor with 9568 × 6380 pixels and a 16-bit A/D converter, and it is equipped with a 100 mm macro lens. The field-of-view necessary to fully cover—perforation area included—the 135 still photography format is 54 × 36 mm. The resulting working distance is ~150 mm and the resolution is 4500 ppi, which is enough to capture the relevant detail of a fine-grain photographic image on film.

Custom printed circuit boards (PCB) were created to properly connect the electrical components that drive the LEDs. A programmable hardware board controlled the status of the PCB, turning the continuous emission of the LEDs on and off.

2.1 Spectral band selection

Ten LEDs were selected whose emissions are evenly distributed in the range of wavelengths that have a considerable contribution for color perception (from 400 to 680 nm) and whose bandwidths result in a limited spectral overlap. The number ten was chosen as it is considered to provide accurate results for colorimetric calculations and spectral reconstruction.[8] It is today possible to find on the market a wide range of LEDs emitting in the visible spectral range with a relatively small bandwidth—FWHM ranging between 15 and 30 nm. However, no LED has a narrow emission with a peak in the region between 530 and 590 nm. To fill this gap, two broad-band LEDs shine through two different interference filters with a FWHM of 20 nm (as depicted by "A" in the diagram of Figure 2). The other eight LEDs have the required actual spectral power distribution (SPD) and directly shine into the integrating sphere (as depicted by "B" in the diagram of Figure 2).

The actual SPD of the light incident on the film ("G" in the diagram of Figure 2) was measured with a spectroradiometer (*Konica Minolta CS-2000*) for each LED. The normalized spectral bands with 1 nm step were calculated multiplying the ten measured SPDs by the values of spectral sensitivity found in the technical specifications of the CMOS sensor. The curves are reported in the left plot of Figure 3, of which the thicker ones represent the standard narrow RGB bands described in the introduction.

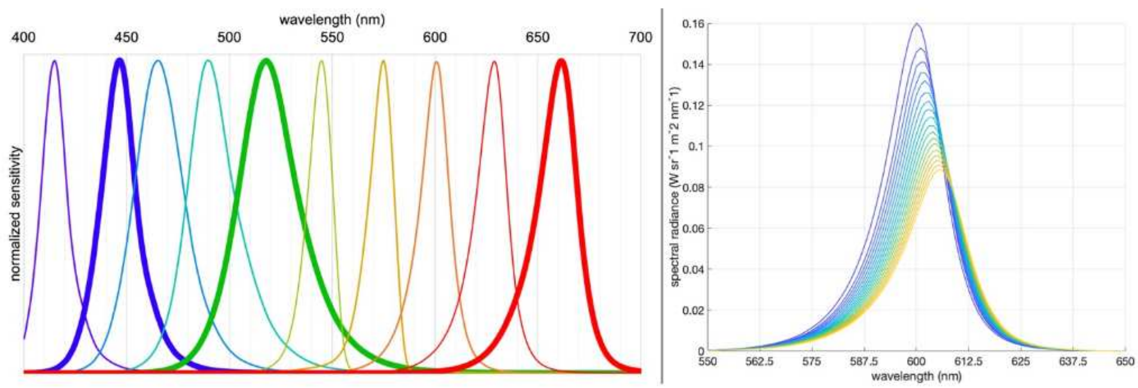

Figure 3. Left: Spectral bands of the multispectral imaging system normalized to have the same maximum value.
Right: Trend of the spectral radiance of the orange LED as the emission time passes and its temperature rises. The color of the curve shifts from blue to yellow as time passes.

The emission of LEDs is known to be temperature-dependent. Despite the LEDs of the multispectral system being equipped with heat sinks, their temperature rose considerably while being on. To assess the instability of the LEDs' emission, their spectral radiance was measured every ten seconds for three minutes. In the three minutes observed, the most unstable of the selected LEDs has an emission peak that shifts from 600 to 606 nm, and its intensity almost halves, as reported in the plot on the right of Figure 3. In the present work, the average spectral radiance of the first twenty second of activity was used in the calculations. Even if the LEDs were only on during the image exposure, some heating up must be considered, especially in case a set of images is captured for each band to increase the signal-to-noise ratio by averaging.

3. IMAGE CAPTURE AND PROCESSING

Before capturing the multispectral images, it is necessary to identify for each LED the integration time that makes the best use of the dynamic range of the sensor and, at the same time, gives a good level of linearity. This is achieved with a routine that tests different integration times with no film sample and quickly finds the longest integration time that does not exceed the ~70% of the sensor's full-well-capacity. Once the optimal integration time is found, the "*white*" image with the LED on and the "*dark*" image with the LED off are captured and stored for all the spectral bands. This calibration procedure must be executed before capturing a film sample each time the system has been reconfigured.

3.1 Transmittance values

A *flat-field* operation is necessary to obtain multispectral images that contains transmittance values. If, due to the thermal instability (Figure 3-right), the raw "*film*" image is captured while the LED emits with a different intensity than while capturing the *white* image, a standard flat-field operation would not provide accurate transmittance values. In view of this, a special flat-field operation was adopted, which exploits the film's perforation. The digital values of the pixels corresponding to the perforation holes in the *film* image ($film_{perf}$) must be the same as the corresponding pixels in the *white* image ($white_{perf}$). This is imposed numerically with the following equation:

$$\mathrm{T} = \frac{\mathrm{film} - \mathrm{dark}}{\mathrm{film_{perf}} - \mathrm{dark}} \cdot \frac{\mathrm{white_{perf}} - \mathrm{dark}}{\mathrm{white} - \mathrm{dark}} \tag{1}$$

The transmittance values resulting from Equation (1) are expressed with 16 bits and stored as ENVI file.[9]

3.2 Color values

Considering transmittance spectra with an interval of 5 nm or less, once an illuminant and an observer are chosen, the CIE recommends computing the tristimulus with the standard summations.[10] In case of transmittance values with lower spectral resolution—such as those from Equation (1)—several deconvolution and interpolation methods have been proposed to reduce the spectral interval and improve the accuracy of the resulting colorimetric values.[11,12] The multispectral images presented in this work consist of ten 16-bit images, each containing 61 megapixels, corresponding to a data cube of over 1.2 GB. With the outlook of using the multispectral imager for motion pictures, thus capturing tens of thousands of data cubes, it is convenient to streamline the computational pipeline.[13] It was decided to test a more agile color calculation that, instead of upsampling the transmittance spectra, downsamples the illuminant and observer functions according to the spectral bands. Considering the [380 780] nanometer range with 1 nm step, $\mathbf{B_N}$ is the 401×10 matrix containing the spectral bands of the multispectral imager (Fig. 3-left) after normalization that sets all their integrals (i.e., vertical sums) equal to one, $\mathbf{S}$ is the 401×1 matrix of the illuminant spectrum and $\mathbf{O}$ is the 401×3 matrix of the color matching functions (CMFs). The 10×1 matrix $\mathbf{S}^*$ and the 10×3 matrix $\mathbf{O}^*$, corresponding to the downsampled illuminant and CMFs respectively, are given by the matrix multiplications

$$\mathbf{S}^* = \left(\mathbf{S}^{\mathrm{t}} \times \mathbf{B_N}\right)^{\mathrm{t}} \quad \text{and} \quad \mathbf{O}^* = \left(\mathbf{O}^{\mathrm{t}} \times \mathbf{B_N}\right)^{\mathrm{t}} \tag{2}$$

Indicating the single column vectors of $\mathbf{O}^*$ with $\bar{\mathbf{x}}^*$, $\bar{\mathbf{y}}^*$ and $\bar{\mathbf{z}}^*$, and $\mathbf{T}$ being the column vector that contains the ten spectral values of transmittance, the tristimulus XYZ is given by

$$\mathrm{X} = \mathbf{T}^{\mathrm{t}} \times (\mathbf{S}^* \circ \bar{\mathbf{x}}^*) \quad , \quad \mathrm{Y} = \mathbf{T}^{\mathrm{t}} \times (\mathbf{S}^* \circ \bar{\mathbf{y}}^*) \quad \text{and} \quad \mathrm{Z} = \mathbf{T}^{\mathrm{t}} \times (\mathbf{S}^* \circ \bar{\mathbf{z}}^*) \tag{3}$$

where the symbol ∘ indicates an element-wise multiplication.

All the color images and values reported in the following section are calculated with the D50 illuminant and the CIE 1931 2° standard observer.[14]

4. EXPERIMENTAL VALIDATION

The optical design of the new imaging system and the computational pipeline were tested on an assorted set of photographic samples. The aim of the new imaging system is to recreate the appearance of film in projection. In view of this, the multispectral captures were compared with spectrally resolved point-based radiometric measurements of the light reflected by a screen during analog projection. The radiometric measurements were taken with the *Konica Minolta CS*-2000 while the samples were projected with a *Leica PRADOVIT P150*. To verify the advantage of the condensed illumination geometry over the diffuse illumination, the multispectral system was tested on a silver-based photographic emulsion containing a grayscale step wedge (Figure 4-left). On the other hand, to verify the appropriateness of the selected spectral bands, the system was tested with an IT8 color chart on *Fuji Provia* reversal film (Figure 4-center). The availability of a series of communicating darkened rooms offered a simple way to reduce the effect of straylight (Figure 4-right), which can significantly affect the radiometric measurements of the dark patches. The film projector (B) was located in a room, projecting the image through an open doorway in a second room. At the focal plane of the projected image, a *Spectralon* disc (C) was reflecting a small portion of the image, while the rest of the rays continued their path and entered a third room through another open doorway. The spectroradiometer (A) measures the spectral radiance reflected by the Spectralon disc, being minimally affected by the light glowing from the film projector and by the light of the whole image radiating in the room that contains the measured surface (room #2). The ratio between the measurement of the projected film and the corresponding measurement without film provides the film transmittance in the specific projection conditions (the dark current is automatically subtracted by the instrument).

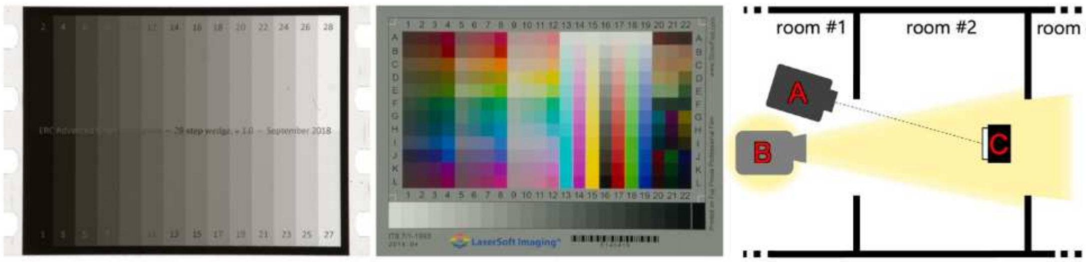

Figure 4. Left: 35 mm grayscale step wedge. Center: IT8 transmissive color chart on Fuji Provia film. Right: Diagram of measurement setup indicating the spectroradiometer (A), the slide projector (B) and the *Spectralon* reflectance disc (C).

4.1 Grayscale step wedge

The grayscale step wedge was captured with the multispectral system in the two illumination conditions ('MSI-diffuse' and 'MSI-condensed') and the transmittance spectra of its twenty-eight steps were measured with the spectroradiometer during analog projection ('projection'). The transmittance values are reported in magenta in the plots of Figure 5. For all the steps, the condensed illumination provides transmittance values that are closer to the analog projection than the diffuse illumination. The patches reported on the right of Figure 5 result from the color calculation described in Section 3.2. They indicate that the projection has 'warmer' grays than both multispectral captures, but the contrast and hue resulting from the condensed illumination are closer to the projection. In fact, the vertical edge between 'projection' and 'MSI-diffuse' stands out more clearly than the edge between 'projection' and 'MSI-condensed'.

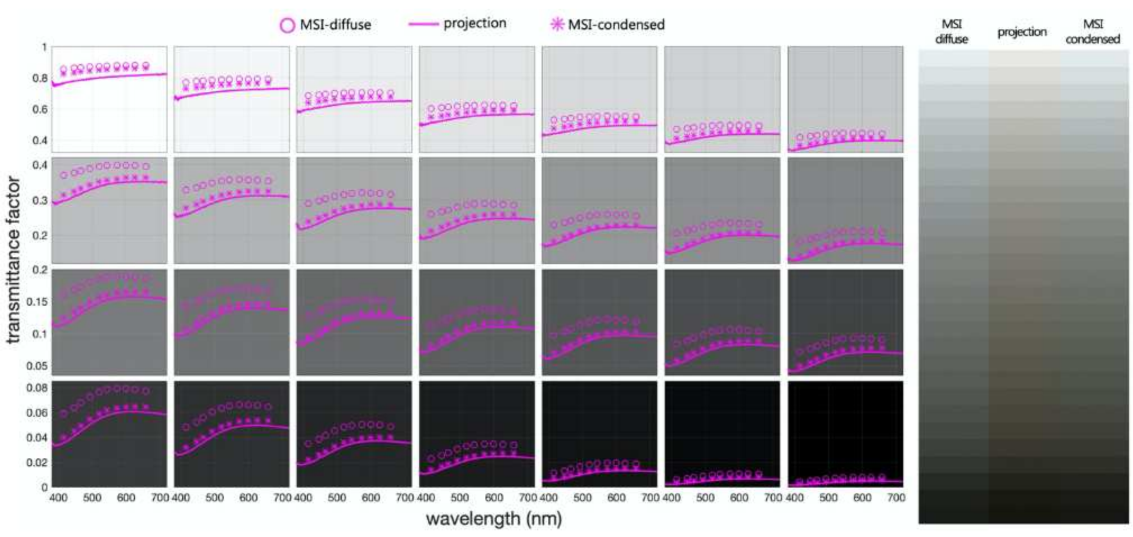

Figure 5. Left: Transmittance values of twenty-eight steps of the grayscale step wedge with three different measuring methods (all the plots in a row have the same transmittance range). Right: Image containing the color of the patches calculated from the reported transmittances.

The residual differences between the transmittance values of 'projection' and 'MSI-condensed' can be ascribed to the diversities in the two measuring setups. In the 'projection' setup, the film is magnified with a ~30X factor, and two photographic objectives with low f-number are employed (by the film projector and by the spectroradiometer). In the 'MSI' setups, on the other hand, the magnification factor is just 1.5X and there is only one photographic objective whose aperture was set to f/11.

4.2 Patches from the IT8 chart

The IT8 chart was captured with the multispectral system in condensed illumination ('MSI') and the transmittance spectra of a selection of ninety-six patches were measured with the spectroradiometer during analog projection ('projection'). Since the chromogenic emulsion constituting the color chart is dye-based and non-scattering, the diffuse and condensed illumination provide the same film's transmittance values,[7] so it is not necessary to distinguish between the two illumination geometries in this case. The comparison between the color values resulting from 'MSI' and 'projection' provides a numerical verification of the appropriateness of the band selection described in Section 2.1 and of the image capture and processing procedure described in Section 3. In Figure 6 the resulting color of the ninety-six patches are reported on the left. Each patch is a square divided in two triangular sections: lower-left corresponds to 'MSI' and higher-right corresponds to 'projection'. The corresponding colorimetric differences are reported on the right of Figure 6 as a heatmap that expresses ΔE2000 values.[15] As it was reasoned for the grayscale step wedge, the residual color differences between 'projection' and 'MSI' can be ascribed to the substantial diversities in the two measuring setups.

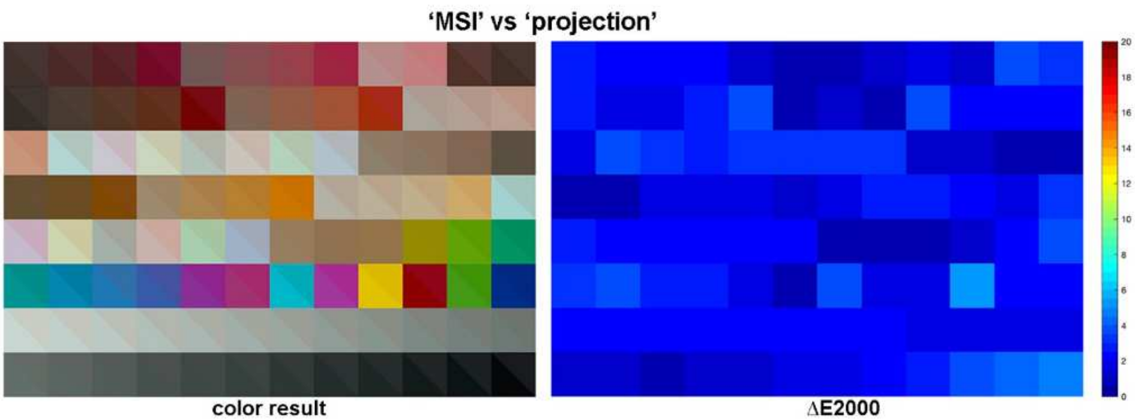

Figure 6. Left: Color of the ninety-six patches of the IT8 target from the multispectral capture (lower-left triangular section) and from the spectroradiometric measurements in projection (higher-right triangular section). Right: Heatmap reporting the colorimetric distances expressed with the ΔE2000 formula.

To numerically assess the advantage of using the multispectral imaging system over conventional film scanners, the result reported in Figure 6 has to be compared with a standard RGB capture. This is done by selecting the narrow RGB bands that are included in the multispectral capture (the thick curves in Figure 3-left) and discarding the other bands. The 'RGB' capture is first compared as it is with 'projection'. In the top diagrams of Figure 7 the resulting color of the ninety-six patches are reported on the left—lower-left triangular sections correspond to 'RGB' and higher-right to 'projection'—while the corresponding colorimetric differences are reported on the right. The RGB capture produces enhanced color saturations that, as discussed in the introduction, may be desirable in some cases (e.g., faded film). However, the resulting image is definitely wrong if the film has to be reproduced with accurate colors.

4.3 Matrix correction

Some methods for the color characterization of film scanners have been proposed in the past.[16,17] Even though these techniques were seldom—if ever—adopted in practice,[2] it is interesting to evaluate to what extent a color managed workflow would improve the results of a narrow RGB scan. A slide containing a *Colorchecker* target[18] was captured with the multispectral system, selecting the narrow RGB bands only. The twenty-four patches of the target were measured with the spectroradiometer during analog projection ('reference'). This training set allowed to calculate a 3-by-3 matrix that minimizes the color difference with the reference, and thus corrects the narrow RGB scan.[19] The comparison between 'RGB' and 'projection' target was repeated for the ninety-six selected patches of the IT8 after the application of the color correction matrix. The result of this comparison is reported in the bottom diagrams of Figure 7. With respect to the results obtained without correction matrix (top diagrams), the exaggerated saturation of the 'RGB' colors is attenuated and the accuracy is overall improved. However, the colors resulting from the multispectral capture (Figure 6) are still significantly better.

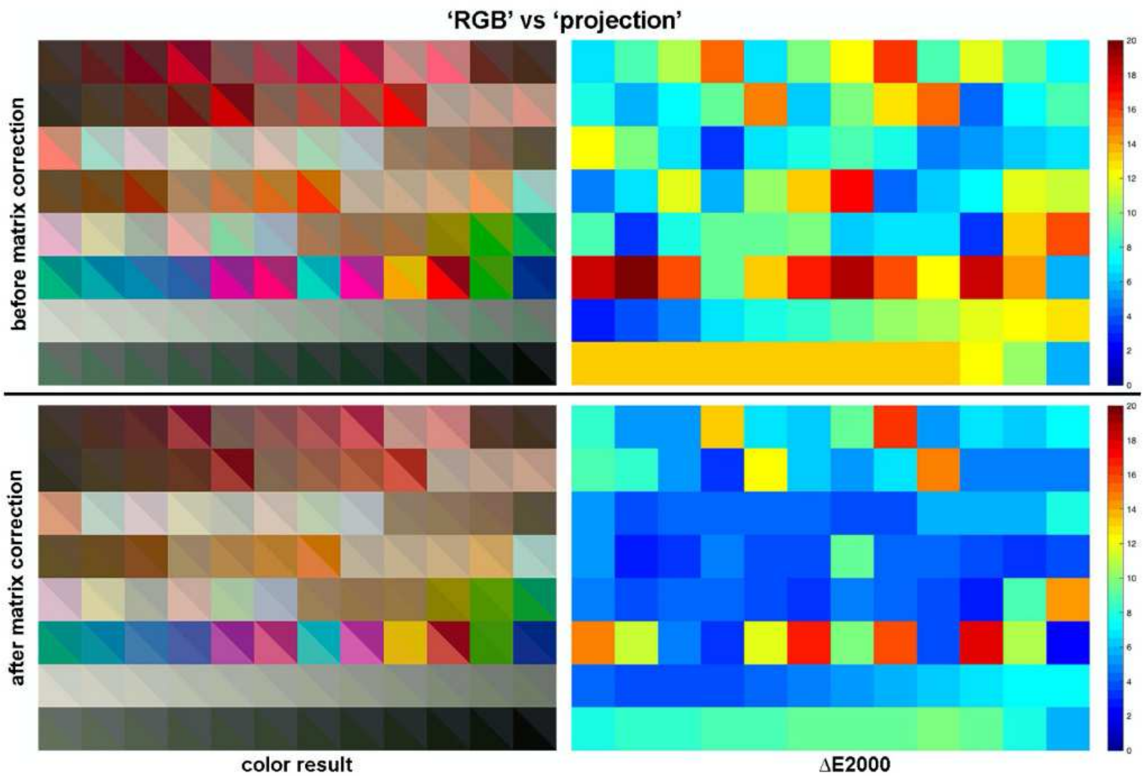

Figure 7. Comparison between the colors resulting from the RGB capture and from the spectroradiometric measurements in projection before (top diagrams) and after the application of the color correction matrix (bottom diagrams). Left: Color of the ninety-six patches ('RGB' is the lower-left triangular section, 'projection' is higher-right). Right: Heatmap reporting the colorimetric distances expressed with the ΔE2000 formula.

5. CONCLUSION

The technical limitation of the digital image capture carried out by conventional film scanners is twofold: on the one hand, the limitation is associated with the diffuse illumination of the film, and on the other hand, with the spectral sensitivities of the RGB capture. To overcome these limitations, a multispectral imaging system was designed and built with a dual condensed/diffuse illumination of the film, which produces the most suitable digital image for all historical film processes. The present work demonstrates that the novel imaging system creates a contrast and chromaticities that are faithful to the visual experience during analog film projection. The novel optical design represents an inexpensive and effective solution for the creation of a new multispectral motion picture scanner prototype.

ACKNOWLEDGEMENTS

The construction of the multispectral imaging system was funded by the project IMATCH from the Norwegian Regional Research Fund (RFF Innlandet) – grant No 298914. Tor Erik Nicolaisen and Monika Skaug Bakkehaug gave support for the 3D modeling and printing, Luvin Munish Ragoo for the electronics, Binu Melit Devassy and Ronny Xavier Velastegui Sandoval for the software. Jean Baptiste Thomas and Julius Muschaweck gave fundamental advice for the optical design. Special thanks go to Sylvie Pénichon who provided the slides for the experiments. The fundamental concept that inspired the work have been developed under the European Union's Horizon 2020 research and innovation programme – grant agreement No 670446 *FilmColors*.

REFERENCES

[1] Flueckiger, B., Pfluger, D., Trumpy, G., Croci, S., Aydın, T. and Smolic, A., "Investigation of Film Material–Scanner Interaction" (2018).

[2] Diecke, J., Trumpy, G., Weiss, M. and Flueckiger, B., "Lea aus dem Süden. Ethical and Practical Considerations for Digital Color Transfer," Journal of Film Preservation 103, 95–101 (2020).

[3] Rudolf Gschwind, Franziska S. Frey, and Lukas Rosenthaler., "Electronic imaging: a tool for the reconstruction of faded color photographs and color movies," Proc. SPIE 2421, Image and Video Processing III 2421, San Jose, CA (1995).

[4] Fossati, G., [From Grain to Pixel. The Archival Life of Film in Transition], Amsterdam University Press, Amsterdam (2009).

[5] Mead, T. W., "Optical scatter correction for film scanners," US 8,009,190 B2 (2011).

[6] Gregory, C. L., "Tinting and Toning Motion Picture Films," [Motion Picture Photography], Falk publishing Company, Incorporated, New York, NY, 177–198 (1927).

[7] Trumpy, G. and Flueckiger, B., "Chromatic Callier Effect and its Repercussions on the Digitization of Early Film Colors," Journal of Imaging Science and Technology 63(1), 10506-1–11 (2019).

[8] R. Shrestha, J. Y. Hardeberg, and C. Boust., "LED Based Multispectral Film Scanner for Accurate Color Imaging," 2012 Eighth International Conference on Signal Image Technology and Internet Based Systems, 811–817 (2012).

[9] "ENVI Header Files.", Harris Geospatial Solutions, 2020, <https://www.l3harrisgeospatial.com/docs/enviheaderfiles.html> (20 May 2021).

[10] "Recommended practice for tabulating spectral data for use in colour computations.", CIE 167:2005, Commission Internationale de l'Éclairage, Vienna (2005).

[11] Hunt, R. W. G. and Pointer, M. R., "Precision and Accuracy in Colorimetry," [Measuring Colour], John Wiley & Sons, Ltd (2011).

[12] A. Mansouri, F. S. Marzani, and P. Gouton., "Neural networks in two cascade algorithms for spectral reflectance reconstruction," IEEE International Conference on Image Processing 2005 2, II–718 (2005).

[13] Darling, B. A., Ferwerda, J. A., Berns, R. S. and Chen, T., "Real-Time Multispectral Rendering with Complex Illumination," Color and Imaging Conference 2011(1), 345–351 (2011).

[14] "Colorimetry — Part 1: CIE standard colorimetric observers.", ISO standard ISO/CIE 11664-1:2019, CIE International Commission on Illumination (2019).

[15] Sharma, G., Wu, W. and Dalal, E. N., "The CIEDE2000 color-difference formula: Implementation notes, supplementary test data, and mathematical observations," Color Research & Application 30(1), 21–30 (2005).

[16] Noriega, L., Morovič, J., MacDonald, L. W. and Lempp, W., "Color Characterisation of a Digital Cine Film Scanner.," The 9th Color Imaging Conference: Color Science and Engineering: Systems, Technologies, Applications, CIC 2001, Scottsdale, AZ, November 6-9, 2001, 239–244 (2001).

[17] Thomas, J.-B. and Boust, C., "Colorimetric Characterization of a Positive Film Scanner Using an Extremely Reduced Training Data Set.," 19th Color and Imaging Conference, CIC 2011, San Jose, CA, November 7-11, 2011, 152–155 (2011).

[18] McCamy, C. S., Marcus, H. and Davidson, J. G., "A color-rendition chart," Journal of Applied Photographic Engineering 2(3), 95–99 (1976).

[19] Bianco, S., Bruna, A. R., Naccari, F. and Schettini, R., "Color correction pipeline optimization for digital cameras," Journal of Electronic Imaging 22(2), 1–11 (2013).